

Catadioptric RGR motion tracking for prospective motion compensation in MR acquisitions

B. S. Armstrong¹, T. P. Kusik¹, R. T. Barrows¹, B. Andrews-Shigaki², J. Maclaren³, M. Zaitsev³, O. Speck⁴, T. Prieto⁵, and T. Ernst²

¹Electrical Engineering, Univ. Wisc.-Milwaukee, Milwaukee, Wisconsin, United States, ²Medicine, University of Hawaii, Honolulu, Hawaii, United States, ³Dept. of Diagnostic Radiology, University Hospital Freiburg, Freiburg, Germany, ⁴Biomedical Magnetic Resonance, Otto-von-Guericke University, ⁵Neurology, Medical College of Wisconsin, Wauwatosa, Wisconsin, United States

Introduction: Subject motion tracking and prospective motion compensation are one means to reduce motion artifacts in MR imaging and spectroscopy [1-5]. Motion tracking methods that have received recent attention include RF coils [5], stereo vision [1-2], and single-camera optical systems [2-3,6]. Optical motion tracking systems offer the advantages of independence from the pulse sequence used and potentially high accuracy, while single-camera systems additionally avoid some of the calibration and line-of-sight challenges of stereo-vision systems [2,3,6]. Single-camera systems include those that operate at short-range, with a camera in the bore and in some cases mounted on the head coil [2,3], and the Retro-grate Reflector (RGR) that can operate with high-accuracy, even when the camera is placed outside the bore. An RGR system that has recently been deployed for prospective motion compensation during MR acquisitions is described.

Materials And Methods: The RGR camera and lighting system in an RF enclosure is seen in Fig 1. The lighting system comprises 8 CREE MC-E quad emitters driven with 1.5 amps for 10,000 lumens of light. RF emission was tested using a high-bandwidth EPI sequence on GE and Siemens 3T scanners without detectable RF interference. In Fig 2, a view from the head end of the scanner shows the custom fabricated rib which supports a mirror. Delrin spars with radial widths of 50 and 30 mm were tested (50 mm shown). With friction material under the feet, the 30mm rib is adequately stiff, and requires less space in the bore. A 100x100 mm mirror is visible, mounted at a 45 degree angle to the axis of the bore. An RGR marker is visible on the rib, another RGR marker is mounted on a phantom and is visible in the mirror. Fig 3 is an image processed by the RGR system. At the working distance of 2.4 meters, the Prosilica GC 650 camera with Schneider 70 mm lens images the 20x20 mm marker with an image size of 65x65 pixels, which is adequate for RGR tracking. Figure 4 shows an RGR marker fixed to a pair of MR-safe goggles. RGR motion data were collected during trials of prospectively-corrected MR imaging, and are analyzed to determine tracking system noise and mirror stability.

Results & Discussion: Results are illustrated in Figs 5-7.

The data in Figs 5 and 6 were collected with the marker on a phantom in the head coil and no motion. For the first half of each trace the scanner is idle, while the second half was acquired during 3D gradient echo imaging. In Fig 5, RMS noise levels are 9 and 8 microns in the RGR X and Y directions, 381 microns in Z, Fig 6 shows Euler angle noise levels below 0.007 degrees on all 3 axes. No change is seen in the noise level at the onset of scanning at t=60 seconds, indicating that the combination of rib and mirror with friction material, and RGR image processing provides robustness to potential vibrations in the scanner. Data collected during a motion-corrected *in vivo* scan is seen in Fig. 7. Motions correspond to an image reported in [6]. To reduce noise impact during imaging, the RGR Z axis (along the camera line-of-sight) was filtered using a 5th order Butterworth filter with $w=0.63$ [rad/sec]. The other position and rotation variables did not require filtering.

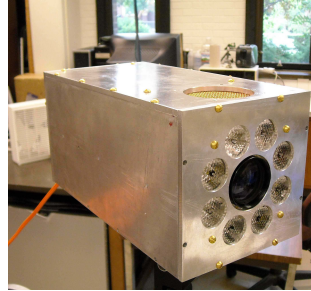


Fig. 1. RGR System in RF enclosure.

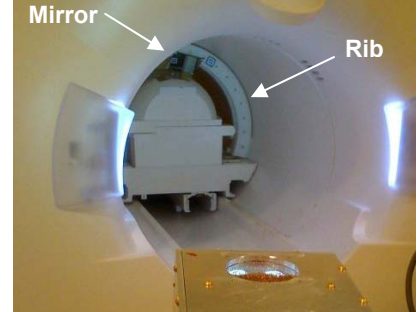


Fig. 2. Head-end of magnet, with camera, rib, mirror & head coil.

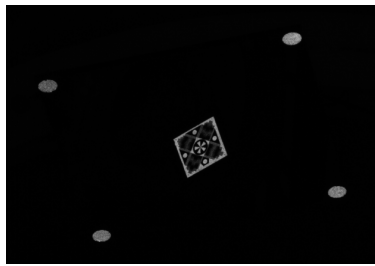


Fig. 3. RGR Marker as seen by camera. Circular retro-reflectors mark mirror corners.



Fig. 4. RGR marker on subject in head coil. Marker viewed by camera via mirror on rib.

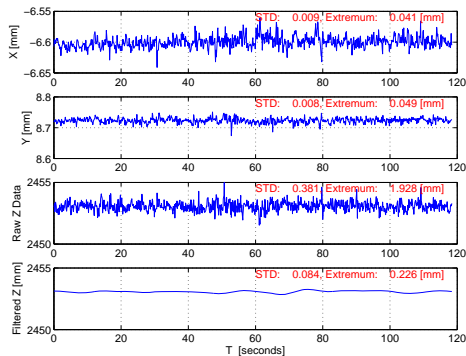


Fig. 5 X Y Z components w/o motion.

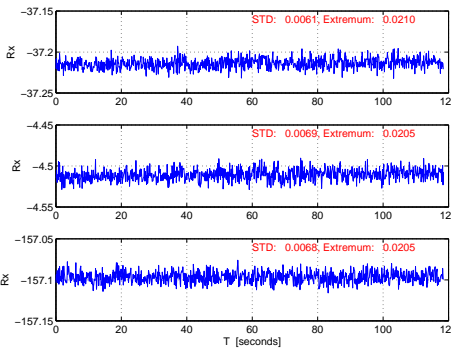


Fig. 6 Rotation components w/o motion.

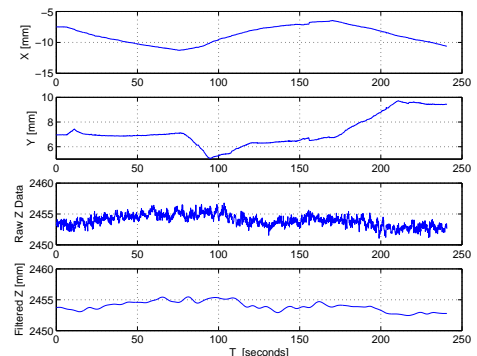


Fig. 7 X Y Z components w/ motion.

References: [1] M. Zaitsev, et al., NeuroImage 2006;31:1038-50; [2] C. Dold, et al., Acad. Radiol. 13(9):1093-1103; [3] M. Aksoy, et al., ISMRM 2009: 04599; [4] L. Qin, et al., ISMRM 2009: 04616; [5] M. B. Ooi ISMRM 2009: 04598; [6] M. Zaitsev, et al., ISMRM 2010; [7] Qin, MRM 62(4):924-934.

Acknowledgements: Grant support from the NIDA (1R01DA021146) and NIAMS (1R15AR0456117) is acknowledged.